Dysregulation of miR-31 and miR-21 Induced by Zinc Deficiency Promotes Esophageal Cancer

Hansjuerg Alder[1,†], Cristian Taccioli[1,†], Hongping Chen[2,†], Yubao Jiang[2], Karl J. Smalley[2], Paolo Fadda[1], Hatice G. Ozer[1], Kay Huebner[1], John L. Farber[2], Carlo M. Croce[1], Louise Y. Fong[2]

[1]The Ohio State University, Columbus, Ohio, USA, [2]Thomas Jefferson University, Philadelphia, Pennsylvania, USA, [†]These authors contributed equally to this work

ABSTRACT

Dietary zinc (Zn) deficiency (ZD) in rats induces an inflammatory gene signature that fuels esophageal squamous cell cancer (ESCC). Using nanoString™ technology, we show that the inflammation is accompanied by altered expression of specific microRNAs in esophagus, as well as skin, lung, pancreas, liver, prostate, and PBMC, predictive of disease development. Particularly, the ZD esophagus has a microRNA signature resembling human ESCC/tongue SCC miRNAomes with overexpression of *miR-31* and *miR-21* and downregulation of their respective tumor suppressor targets PPP2R2A and PDCD4. Esophageal *miR-31* and *miR-21* levels are directly associated with the appearance of ESCC. In situ hybridization localizes *miR-31* to tumor and *miR-21* to stromal cells, establishing their cell-type specificity. In regressing tongue SCCs from Zn-supplemented rats, *miR-31* and *miR-21* expression was concomitantly reduced, establishing their responsiveness to Zn-therapy. A search for putative microRNA targets revealed a bias toward genes in inflammatory pathways. Thus, ZD induces inflammation-associated microRNAs and promotes ESCC[1].

INTRODUCTION

ESCC is a deadly cancer with a 5-year survival of ~10%. The major risk factors are alcohol consumption, tobacco use, and nutritional deficiencies, including ZD. Zn is an essential trace element required for the activity of >300 enzymes, for proper immune function, and for the conformation of >2000 transcription factors that control cell proliferation, apoptosis, and signaling pathways. ZD predisposes to diseases by adversely affecting these processes.

Our ZD rat tumor model that reproduces the ZD link to human ESCC provides an opportunity to decipher the mechanism by which ZD promotes ESCC. Previously, we showed that weanling rats on a ZD diet for 6 weeks developed a precancerous upper aerodigestive tract (tongue, esophagus, and forestomach [expanded lower esophagus]), with increased cellular proliferation and extensive gene expression changes, including overexpression of proinflammation-genes *S100a8* and *S100a9*[2]. Prolonged ZD (~21 weeks) amplified this inflammation by causing overexpression of numerous inflammation genes in addition to *S100a8/S100a9*, thereby providing an inflammatory microenvironment conducive to ESCC development upon repeated exposure to an environmental carcinogen. Zn-replenishment (ZR) reversed the inflammatory signature and prevented cancer formation[3]. In nutritionally complete rats, Zn-supplementation suppressed tongue SCC development by attenuating inflammation[4].

microRNAs (miRNAs) are small non-coding RNAs that have emerged as powerful posttranscriptional regulators of gene expression. The ability of individual miRNAs to regulate a large number of mRNA species allows them to coordinate complex programs of gene expression that alter critical biological processes such as proliferation, apoptosis, and signaling events[5]. miRNAs expression levels are altered in many human cancers[6] and chronic inflammatory diseases/conditions[7].

Here we investigated whether overexpression of cancer-related inflammation genes induced by ZD in the esophagus[3] is a consequence of a protumorigenic microRNA signature. We examined miRNA profiles in esophagus and six other tissues (skin, lung, pancreas, liver, prostate, peripheral blood mononuclear cells [PBMC]) after prolonged ZD, using the nanoString nCounter technology[8,9].

METHODS

Study design: Male weanling Sprague-Dawley rats were fed an egg white-based ZD or Zn-sufficient (ZS) diet for 23 weeks[1]. Blood, esophagus, tongue, skin, lung, liver, prostate, and pancreas were collected. Esophagus and tongue were cut into two portions: one portion was formalin-fixed and paraffin-embedded (FFPE) and the other snap-frozen and stored at -80°C.

miRNA expression profiling: The nanoString nCounter system (nanoString Technologies) that directly measures miRNA expression levels without enzymatic reactions or bias was used. Total RNA (100 ng) was the input material. Small RNA samples were prepared by ligating a specific DNA tag onto the 3′ end of each mature miRNA. The tags provided identification for each miRNA species in the sample. Following hybridization with a panel of miRNA:tag-specific nCounter capture and barcoded reporter probes, the hybridized probes were immobilized on a streptavidin-coated cartridge. Fluorescent barcodes and target RNA molecules were quantified and a high-density scan was performed. Each sample was normalized to the geometric mean of 50 most highly expressed miRNAs. Statistical significances of pair-wise comparisons were calculated by student's t-test.

Gene ontology (GO) analysis: For each miRNA, the common target genes found in >2 databases (RNAhybrid, TargetScan, miRDB and microRNA.org) were used. GO analysis was performed using Database for Annotation, Visualization and Integrated Discovery (DAVID).

TaqMan miRNA assay: Pre-designed probes and U87 (normalizer) were from Applied Biosystems, and the comparative Ct method was used.

In situ hybridization (ISH): FFPE sections were hybridized with double DIG-labeled locked nucleic acid (LNA) detection probes: antimiR-31, antimiR-21 or mismatch probes (Exiqon) in hybridization buffer (57°C for 14 h). The sections were then blocked against unspecific binding of the detecting antibody. miRNA was localized by incubation with 4-nitro-blue tetrazolium (NBT) and 5-brom-4-chloro-3Ý-indolylphosphate (BCIP), and counterstained by nuclear fast red.

Immunohistochemistry (IHC): PDCD4 (LS-B1388, Lifespan Biosciences) IHC was performed on FFPE sections after antigen retrieval[3].

Immunoblot Analysis: Protein samples were separated by SDS-polyacrylamide gel electrophoresis. The primary antibodies used were: PDCD4, TPM1 (ab55915; Abcam), PPP2R2A (#5689, Cell Signaling). RHOBTB1 (sc-102084; Santa Cruz Biotech), STAU2 (sc-87439; Santa Cruz Biotech). Immuno-detection was by Pierce enhanced chemiluminescence substrate.

RESULTS

Figure 1. Normal ZS organs display high abundance of tissue-specific microRNAs.

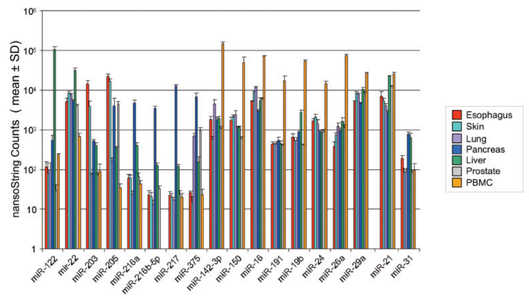

ZS organs show high abundance of liver-specific *miR-122* in liver; skin-specific *miR-203* in skin; epithelia-specific *miR-205* in skin and esophagus; pancreas-specific *miR-375*, *miR-216*, *miR-217* in pancreas; hematopoietic markers *miR-142-3p*, *miR-150*, *miR-16*, *miR191*, *miR-26a*, *miR-19b* in PBMC. These data establish that nanoString system is sensitive and specific.

Figure 2. ZD induces distinct microRNA expression patterns in a wide variety of tissues.

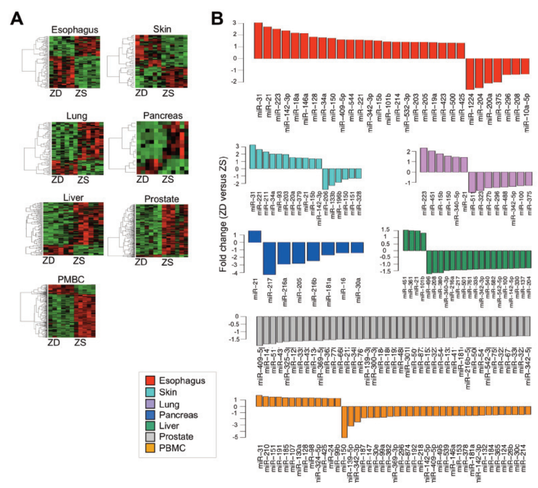

(A) Heat maps showing supervised clustering of miRNA expression in 7 tissues (n=6 rats/dietary group/tissue, P<0.05). **(B)** Barplots showing fold-change of miRNA expression in ZD vs ZS tissues (P< 0.05, fold change ≥ 1.3).

Figure 3. Taqman miRNA assay validates nanoString data.

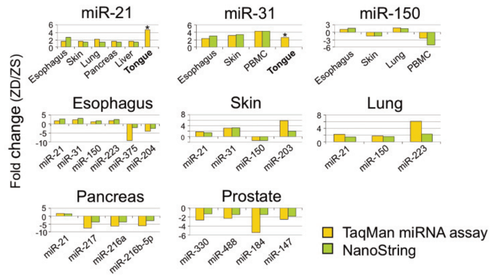

TaqMan miRNA assay validates 14 representative miRNAs in ZD tissues and establishes upregulation of *miR-31* and *miR-21* in ZD tongue.

Table 1. ZD rat tissues show dysregulated oncogenic/tumor suppressor microRNAs that are aberrantly expressed in various human diseases.

ZD esophagus (Human ESCC/oral SCC)
↑ *miR*-31, *miR*-21, *miR*-223, *miR*-142-3p, *miR*-221;
↓ *miR*-204, *miR*-375

ZD skin (Psoriasis)
↑: *miR*-31, *miR*-21, *miR*-142-3p

ZD lung (COPD/Human lung cancer)
↑: *miR*-223, *miR*-451, *miR*-15b, *miR*-21

ZD pancreas (Human pancreatic ductal adenocarcinoma)
↑: *miR*-21
↓: *miR*-217, *miR*-216a, *miR*-216b-5p (pancreas-specific)

ZD liver (Human hepatocellular cancer)
↑: *miR*-21

ZD prostate (Human prostate cancer)
↓: *miR*-184, *miR*-488, *miR*-330

ZD PBMC (Serum of ESCC patients)
↑: *miR*-31

ZD PBMC (Serum of patients with sepsis)
↓: *miR*-150

↑ Upregulated ↓ Downregulated

Figure 4. *miR-31* and *miR-21* overexpression in precancerous ZD esophagus/tongue is cell type specific.

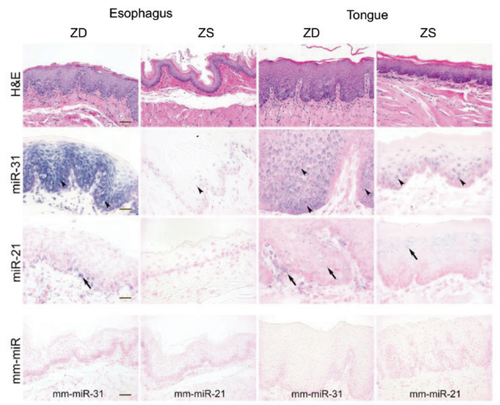

miR-31 ISH signal (blue, NBT/BCIP, arrowheads) was strong/abundant in esophageal/tongue epithelia of ZD vs ZS tissues, *miR-21* signal (blue, arrows) moderate in basal/stromal cells in ZD vs ZS tissues. mm-*miR-31* or mm-*miR-21* (2 mismatches) had no ISH signals. Scale bar, 25 µm.

Figure 5. Overexpression of *miR-31* and *miR-21* is associated with downregulation of their tumor-suppressor targets.

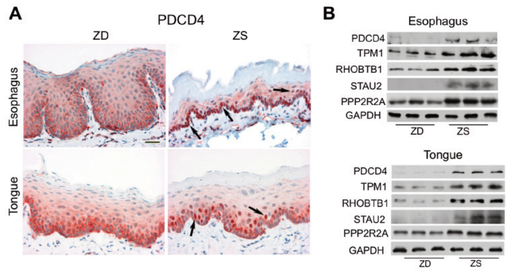

(A) IHC shows reduction of PDCD4 (target of *miR-21*) nuclear expression in ZD esophagus/tongue vs ZS tissues. **(B)** Immunoblots show downregulation of PDCD4 and TPM1 (targets of *miR-21*), RHOBTB1, STAU2, and PPP2R2A (targets of *miR-31*) in ZD esophagus/tongue vs ZS tissues.

Figure 6. Correlation of *miR-31* and *miR-21* expression and ESCC outcome in Zn-modulated rats[3].

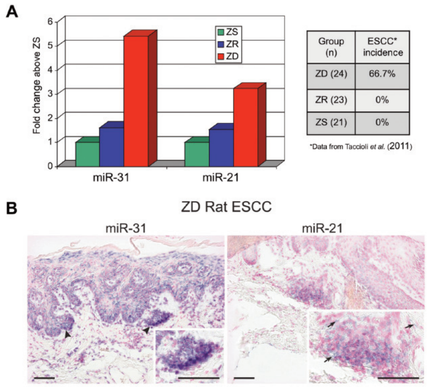

Group (n)	ESCC* incidence
ZD (24)	66.7%
ZR (23)	0%
ZS (21)	0%

*Data from Taccioli et al. (2011)

(A) Taqman miRNA assay: *miR-31* and *miR-21* expression levels are 5.4 and 3.2-fold higher in ESCC-bearing ZD esophagi vs cancer-free ZS controls. ZR that prevented ESCC development[3] reduces miR-31 and *miR-21* expression to ZS levels. **(B)** ISH assay: strong/abundant *miR-31* signal (blue, NBT/BCIP, arrowheads) in tumor and *miR-21* signal (blue, arrows) in stroma of ESCC from a ZD rat; weak/absent *miR-31/miR21* signals in ZS and ZR esophageal samples.

Figure 7. *miR-31* and *miR-21* expression in tongue SCCs is responsive to Zn-therapy.

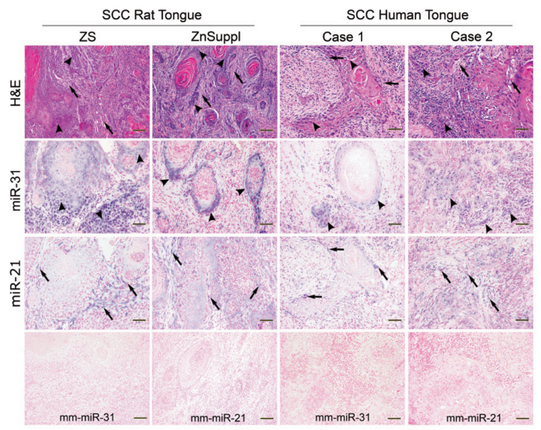

SCC rat tongue: We investigated if Zn-supplementation that suppresses tongue cancer development and attenuates inflammation4 also reduces *miR-31* and *miR-21* expression. In tongue SCCs without Zn therapy, *miR-31* and *miR-21* expression was strong/abundant in tumor and stroma, respectively (*miR-31*: blue, arrowheads; *miR-21*: blue, arrows). In tongue SCCs with Zn therapy, ISH signals of both oncomiR were reduced in intensity and scope, establishing that their expression was responsive to Zn-therapy.

SCC human tongue (H&E): *miR-31* signal was localized to tumor cells (blue, arrowheads), and *miR-21* to stroma (blue, arrows). mm-*miR-31* or mm-*miR-21* (2 mismatches) showed no signals.

Figure 8. Prolonged ZD (23 weeks) reduces tissue Zn content and induces overexpression of inflammation markers.

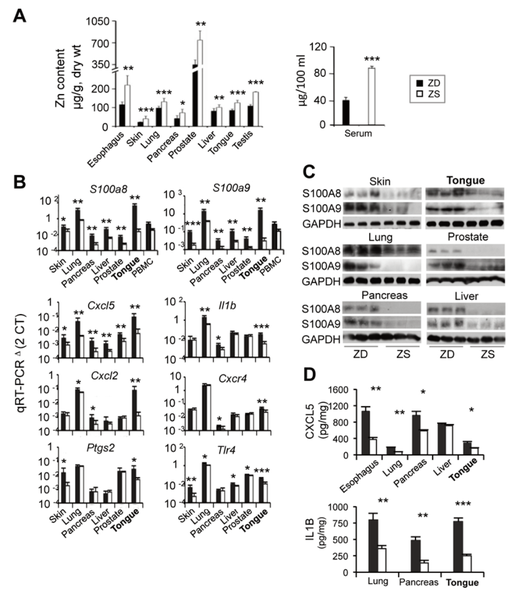

(A) Serum and tissue Zn content. **(B)** qRT-PCR analysis of 8 inflammation genes (normalized to PSMB6) (ZD vs ZS, *P<0.05, **P<0.01, ***P<0.001). (C, D) Expression of inflammation proteins: immunoblot (S100A8 and S100A9); ELISA assay (CXCL5 and IL1B).

Table 2. Gene ontology (GO) enrichment analysis of the microRNA target genes in Zn-deficient tissues.

ZD Tissue	GO terms	No. of genes	En* Score	Adjusted *P*-value
Esophagus	Zn ion binding family	119	3.4	0.010
	Positive regulation of cell differentiation	67	2.9	0.011
	Serine/threonine-protein kinase 10 family	59	1.8	0.021
	MAPKK and JNK family	42	1.4	0.041
	Negative regulation of actin filament family	31	1.3	0.042
	Epithelial cell proliferation	22	0.9	0.049
Skin	ATP calmodulin pathway	56	4.1	0.018
	Actin and ubiquitin regulation	24	2.1	0.023
	Zn ion binding proteins	18	1.0	0.044
Lung	Transcription regulation by RNA-pol II	187	3.1	0.015
	Negative regulation of biosynthesis pathways	103	2.9	0.012
	Zn ion binding family	68	1.4	0.037
	Lung development	23	1.0	0.046
Pancreas	Positive regulation of anti-apoptosis genes	79	2.1	0.024
	Insulin signal pathway	68	1.2	0.035
	Zn ion binding proteins	20	0.9	0.046
Liver	Zn ion binding family	101	4.1	0.023
	Glicosyl-lysin family	93	2.1	0.028
	Post-transcription regulation	49	1.7	0.033
Prostate	Magnesium metabolism family	77	6.4	0.021
	ATP biosynthetic process	63	5.5	0.022
	Endocytosis	39	4.9	0.033
	Transcription regulatory activity	21	3.4	0.036
	TGB-beta signaling pathway	22	2.0	0.040
	Zn finger domain family	19	1.4	0.046
PBMC	Zn finger family	115	3.0	0.035
	Ubiquitin-conjugating enzyme	82	2.8	0.039
	Proteolysis - cellular protein catabolic process	79	1.7	0.040
	Protein-lysine-N-methyltransferase activity	62	1.4	0.045

*Enrichment Score

CONCLUSIONS

This study shows that prolonged dietary ZD induces aberrant microRNA expression in a wide variety of tissues associated with inflammation, suggesting a likely mechanism contributing to the burden of human diseases associated with ZD. Importantly, the demonstration of the dysregulation of *miR-31* and *miR-21* by dietary ZD in inflammatory esophageal/lingual neoplasia provides new insight into the mechanisms whereby ZD promotes human ESCC and tongue SCC.

This work was supported by NIH grants (R01CA118560, R21CA152505 to L.Y.F. and R01CA115965 to C.M.C.).

REFERENCES

1 Alder, H. et al. Dysregulation of miR-31 and miR-21 induced by zinc deficiency promotes esophageal cancer. *Carcinogenesis* **33**, 1736-1744 (2012).
2 Taccioli, C. et al. Zinc replenishment reverses overexpression of the proinflammatory mediator S100A8 and esophageal preneoplasia in the rat. *Gastroenterology* **136**, 953-966 (2009).
3 Taccioli, C. et al. Dietary zinc deficiency fuels esophageal cancer development by inducing a distinct inflammatory signature. *Oncogene* **31**, 4550-4558, (2012).
4 Fong, L. Y. et al. Zinc supplementation suppresses 4-nitroquinoline 1-oxide-induced rat oral carcinogenesis. *Carcinogenesis* **32**, 554-560 (2011).
5 Bartel, D. P. MicroRNAs: target recognition and regulatory functions. *Cell* **136**, 215-233 (2009).
6 Calin, G. A. & Croce, C. M. MicroRNA signatures in human cancers. *Nat Rev Cancer* **6**, 857-866 (2006).
7 Schetter, A. J., Heegaard, N. H. & Harris, C. C. Inflammation and cancer: interweaving microRNA, free radical, cytokine and p53 pathways. *Carcinogenesis* **31**, 37-49 (2010).
8 Geiss, G. K. et al. Direct multiplexed measurement of gene expression with color-coded probe pairs. *Nat Biotechnol* **26**, 317-325 (2008).
9 Wyman, S. K. et al. Post-transcriptional generation of miRNA variants by multiple nucleotidyl transferases contributes to miRNA transcriptome complexity. *Genome Res* **21**, 1450-1461 (2011).